

# Effect of modification and ceramic particles on solidification behavior of aluminum-matrix composites

SHUSEN WU

*State Key Lab of Dies Technology, Huazhong University of Science and Technology, Wuhan (430074), People's Republic of China*  
E-mail: wushusen@public.wh.hb.cn

YA YOU

*Kimura Foundry Co., Ltd., Shizuoka (411), Japan*

PING AN

*State Key Lab of Dies Technology, Huazhong University of Science and Technology, Wuhan (430074), People's Republic of China*

T. KANNO

*Kimura Foundry Co., Ltd., Shizuoka (411), Japan*

H. NAKAE

*Department of Materials Science and Engineering, Waseda University, Tokyo (169), Japan*

Thermal analysis is used to establish the relationship between solidification history and the microstructure of SiC particulate reinforced Al-Si alloy-matrix composites. The results show that cooling curves are influenced by the presence of SiC particles and by strontium modification. The eutectic growth temperature of SiC<sub>p</sub>/359 composites modified with Sr lies in the range of 840 to 843 K, i.e., about 5 to 7 K higher than that of Sr-modified unreinforced 359. For the same composite, the eutectic undercooling is higher with Sr modification than without. The eutectic solidification time of the composites is shorter than that of the unreinforced base alloy because of the presence of the ceramic particles. Strontium modification has the tendency to extend the eutectic solidification time. Microstructure analysis reveals that Sr modification has a refining effect on eutectic silicon for the composites, and SiC particles in the composite melt serve as the substrates for eutectic Si phase nucleation. © 2002 Kluwer Academic Publishers

## 1. Introduction

Silicon-carbide particulate-reinforced aluminum-matrix composites have been gaining wide acceptance in automotive and aircraft industries. One of the most important processes to fabricate the metal-matrix composites (MMCs) is liquid-metal casting. The composite microstructure and mechanical properties are influenced by modification of the melt and the solidification process. Because of the presence of ceramic particulates in the melt, the solidification of composites can be quite different from that of traditional alloys [1, 2]. Geometrical restrictions and capillary phenomena caused by the reinforcement can result in alterations of matrix coarsening, microsegregation, tip undercooling, and final solidification structure [3, 4].

Cooling curve analysis has been used to determine the occurrence of various phases during the solidification of nonferrous alloys [5, 6]. The arrest points in the cooling curve are characteristic of transformations and

reactions occurring in a given alloy system. Analysis of these characteristic parameters permits the foundryman to monitor, regulate, and optimize the melt chemistry before an actual casting is made.

In the present study, the effects of strontium modification on the solidification parameters of SiC<sub>p</sub>/Al-Si composites, such as freezing time and eutectic undercooling, have been investigated by using the thermal analysis method. The effects of particulate amount on solidification behavior and microstructure have also been studied. The matrix material composition of the composites is that of 359, and this alloy is therefore included in the present study as a reference material.

## 2. Experimental procedures

Three Al-Si alloy materials were used for the thermal analysis, the compositions of which are shown in Table I. One is the 359 base alloy material. The two

TABLE I Chemical composition of the materials (wt%)

Alloys	Si	Mg	Cu	Fe	Ti	Sr <sup>a</sup>
359	9.32	0.48	0.05	0.18	0.08	0.060
10% SiC/359	9.25	0.47	0.03	0.15	0.09	0.051
20% SiC/359	9.20	0.45	0.02	0.11	0.10	0.052

<sup>a</sup>For the modified ones.

composites are of 14 μm SiC particulate reinforced 359, one with 20vol% SiC (volume percent), another with 10vol% SiC. The DURALCAN composites F3S20S(359 aluminum-silicon alloy reinforced with 20vol% SiC particles) was used as master material for making the 10vol% SiC composite by dilution. For matrix modification, strontium was added with an Al-10wt% Sr master alloy.

The materials were melted in an electrical resistance-heated furnace. The melt was degassed with Ar gas bubbling. Since SiC particles tend to settle at the bottom, the composite melt was stirred for 5 minutes using a graphite impeller in order to produce a homogeneous distribution of SiC particles in the melt. The composites were poured into the mold immediately after stirring, with or without strontium modification. The pouring temperature was maintained throughout the study at 1003 ± 5 K.

The sampling mold was a cylindrical resin-bonded sand mold with a 34 mm diameter and a 70 mm height. The cooling curves were obtained by recording the temperature variation as a function of time of solidification, with a NiCr-NiSi thermocouple and a recorder. The thermocouple was always positioned at the same distance of 30 mm from the bottom of the mold center. The data were also transferred to a computer for analysis. All the cooling curves were obtained under the same conditions. After cooling to room temperature, the samples were sectioned at locations close to the thermocouple, polished, and etched for microstructural observations.

### 3. Results

#### 3.1. Characteristics of primary crystallization

The thermal analysis parameters are indicated in Fig. 1 and defined as follows.

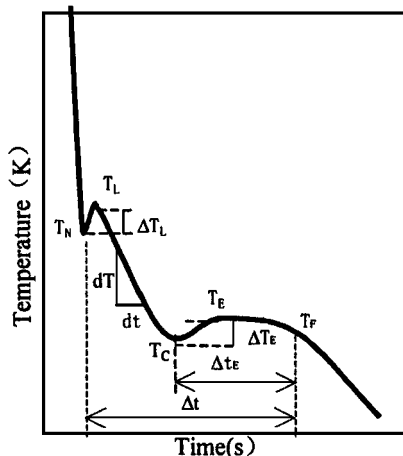


Figure 1 Representation of characteristic thermal analysis parameters.

- $T_N$ : nucleation temperature of primary  $\alpha$  phase;
- $T_L$ : liquidus arrest temperature;
- $\Delta T_L$ : liquidus undercooling,  $\Delta T_L = T_L - T_N$ ;
- $T_C$ : eutectic nucleation temperature;
- $T_E$ : eutectic growth temperature;
- $T_F$ : end temperature of eutectic reaction;
- $\Delta T_E$ : eutectic undercooling,  $\Delta T_E = T_E - T_C$ ;
- $\Delta t_E$ : eutectic solidification time;
- $\Delta t$ : total solidification time;
- $\frac{dT}{dt}$ : cooling rate.

Cooling curves obtained in the experiment are shown in Fig. 2a and b, in which (a) indicates the cooling curves of the three unmodified materials, and (b) that of modified materials. The first peak of the cooling curves represents the formation of primary phase, the second that of the eutectic.

#### 3.1.1. Liquidus arrest temperature

The liquidus temperatures ( $T_L$ ) of the six systems are plotted in Fig. 3. It is seen that the liquidus temperatures

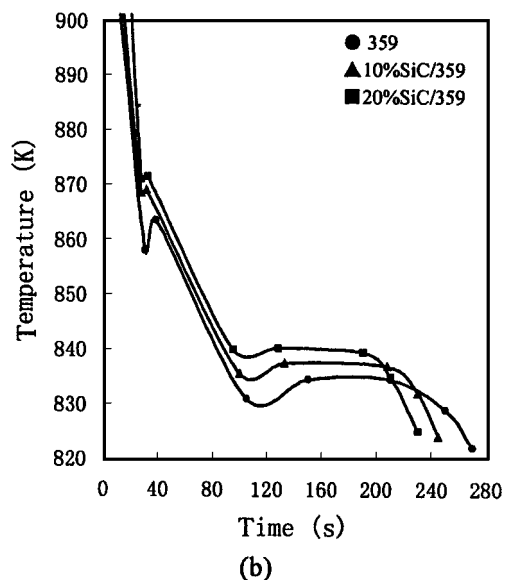
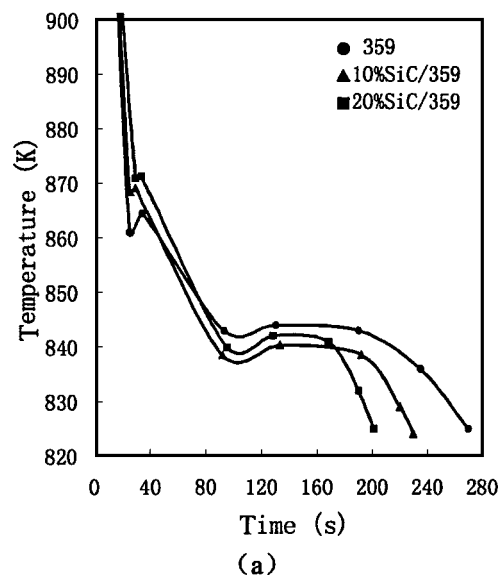


Figure 2 Cooling curves obtained, (a) unmodified, (b) modified with Sr.

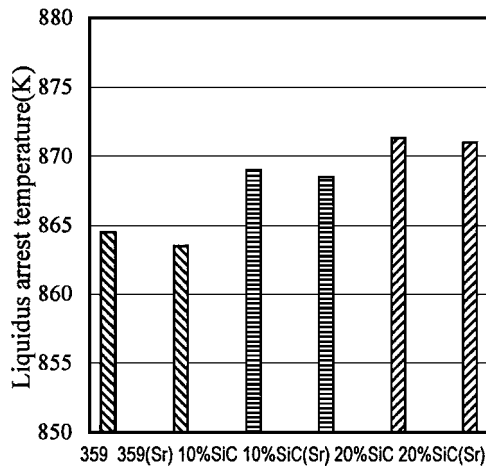


Figure 3 Comparison of liquidus temperature  $T_L$ .

of the composites are higher than those of the corresponding unreinforced matrices. The higher the volume content of SiC particles, the higher the liquidus temperature. From Table I we know that the matrix of the composites is somewhat leaner in silicon content than the 359 alloy. This is also expected to have some effect to raise the liquidus temperature of the composites. For the same material, Sr modification has little effect on the liquidus temperature, which indicates that strontium does not influence formation of the primary  $\alpha$  phase of Al-Si alloys.

### 3.1.2. Liquidus undercooling

The liquidus undercooling  $\Delta T_L$ , the difference between liquidus arrest temperature ( $T_L$ ) and nucleation temperature ( $T_N$ ) of primary  $\alpha$  phase, of the six materials are shown in Fig. 4. It is clear that liquidus undercooling of the composites is much smaller than those of the base metals. It can also be concluded from the cooling curves that the solidification time of the primary phase of the 359 alloy is longer than that of SiC/359 composites.

## 3.2. Characteristics of eutectic solidification

### 3.2.1. Eutectic growth temperature

The eutectic growth temperatures ( $T_E$ ) of the studied materials are plotted in Fig. 5. It is seen that  $T_E$  of un-

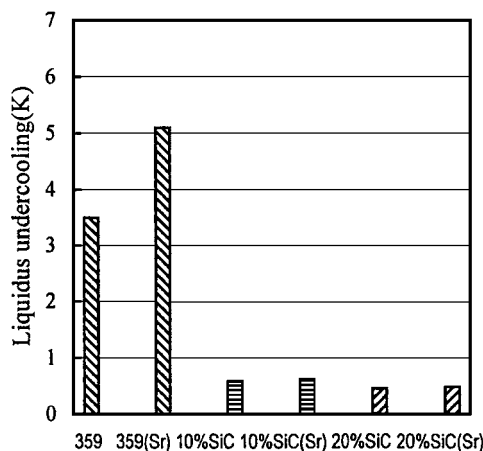


Figure 4 Plot of liquidus undercooling  $\Delta T_L$ .

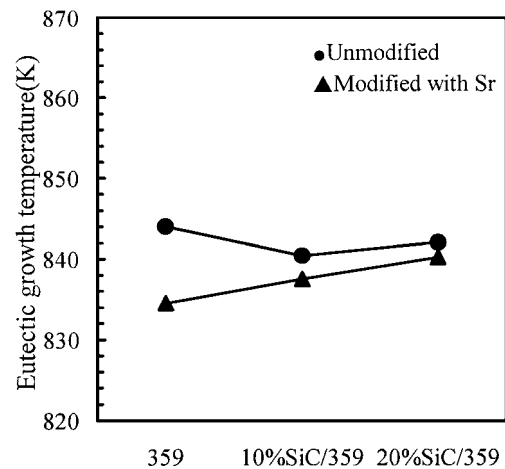


Figure 5 Plot of eutectic growth temperature  $T_E$ .

modified 359 is the highest and that of modified 359 is the lowest, and the difference is about 9 K. This is expected, as a main feature of Sr modification is a decrease of the eutectic temperature [7, 8]. The eutectic growth temperatures of modified SiC/359 composites are about 4 K higher than that of modified 359. With an increase of SiC content, from 10vol% to 20vol%, the eutectic growth temperature increases, whether modified or not. A lower eutectic growth temperature usually means finer eutectic microstructures.

From cooling curves in Fig. 2 it is also seen that the eutectic undercooling ( $\Delta T_E$ ) of the modified base alloy is higher than those of modified composites.

### 3.2.2. Eutectic solidification time

For the Al-Si base alloy, the eutectic solidification time ( $\Delta t_E$ ) is extended by strontium modification (Fig. 6). However, because of the presence of SiC particles,  $\Delta t_E$  of the composites is much shortened. For the same composite, e.g. 20vol% SiC/359 composite, Sr modification also extends the eutectic solidification time.

The total solidification time ( $\Delta t$ ) is defined as the time interval between the start of solidification and end of eutectic reaction. It has the same evolution as  $\Delta t_E$ , as shown by cooling curves in Fig. 2.

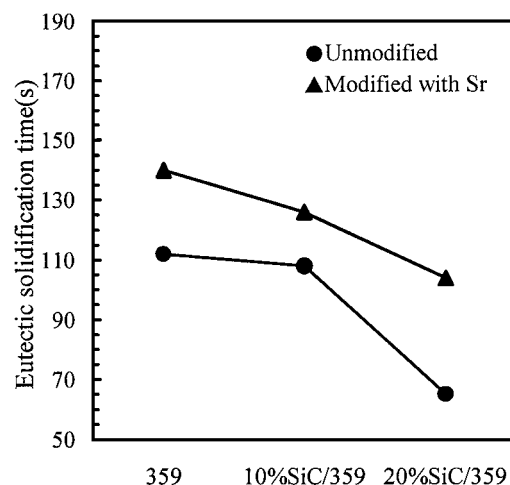


Figure 6 Comparison of eutectic solidification time  $\Delta t_E$ .

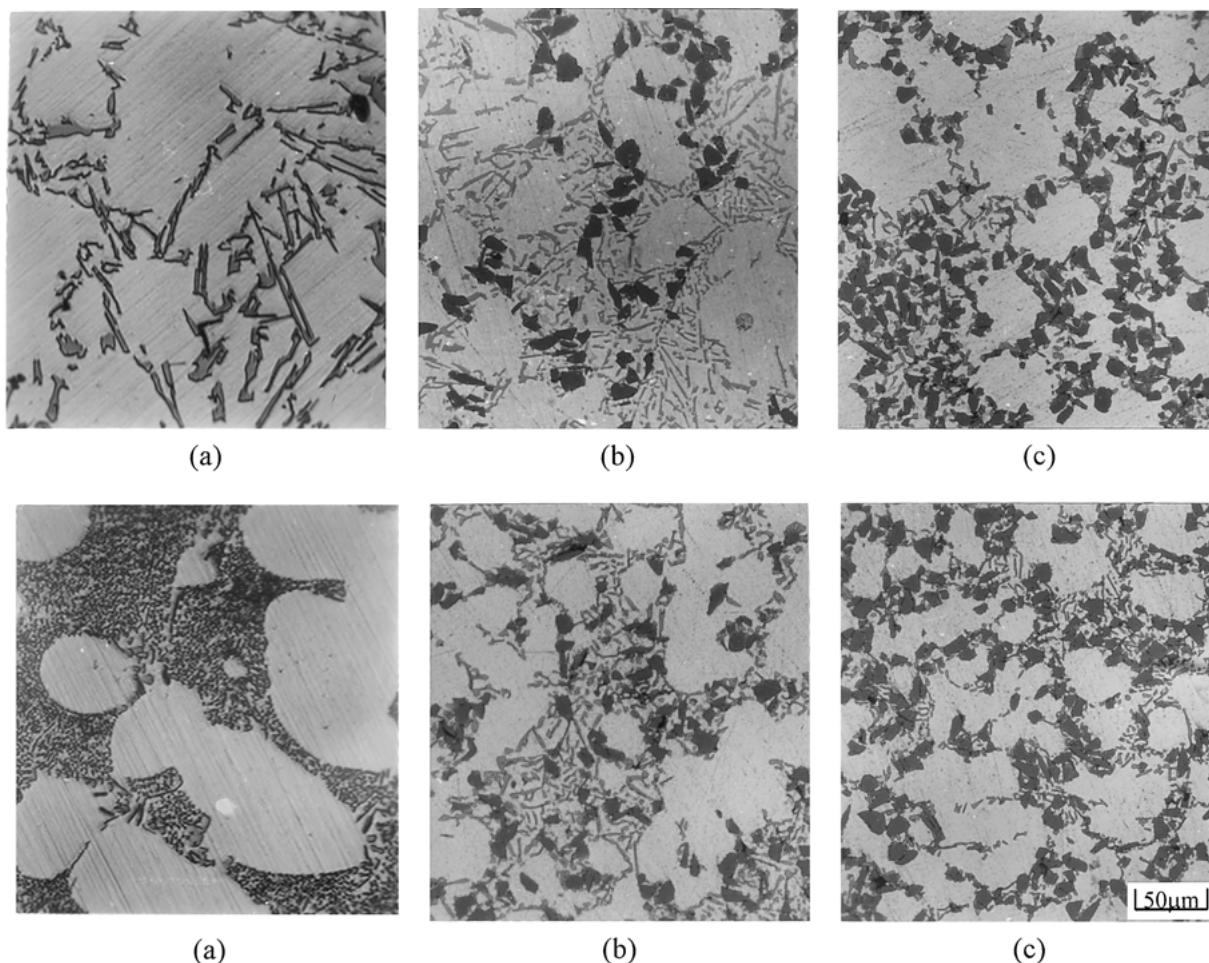


Figure 7 As-cast microstructure of (a) 359, (b) 10% SiC/359, and (c) 20% SiC/359 (Above: unmodified; below: modified with Sr).

### 3.2.3. Microstructures

The as-cast microstructures of the three alloys under different treatment are shown in Fig. 7, in which unmodified materials are above, modified ones at below. The dendrite arm spacing (DAS) of 359 is from 70  $\mu\text{m}$  to 100  $\mu\text{m}$ , and DAS of the composites is from 50  $\mu\text{m}$  to 70  $\mu\text{m}$ . The more the SiC particles, the smaller the DAS.

For the eutectic microstructures, Sr modifies the eutectic Si whether in 359 or the composites, as shown in Fig. 7. The modified eutectic Si phases are much finer than those of the unmodified ones.

The distribution of SiC particles in the composites is mainly between dendrite arms, i.e., particles are pushed by primary  $\alpha$  dendrites and gathered at eutectic zones. The SiC particles are not uniformly distributed in solid matrix. If the cooling rate is faster, e.g. in a metallic mold, the distribution of SiC particles will be macroscopically more uniform [8, 9].

## 4. Discussion

### 4.1. Effect of SiC particles on solidification behavior

The solidification behavior of SiC particulate reinforced Al-Si alloy-matrix composites described above could be explained knowing the thermophysical properties of the composites. The studied composites (c) consist of two components: the matrix metal (m) and the ceramic particles (p). These components differ

in thermal conductivity ( $\lambda_m, \lambda_p$ ), specific heat ( $c_m, c_p$ ) and density ( $\rho_m, \rho_p$ ). Usually composites have varying contents of ceramic particles ( $V_p$ ) in the volume of casting ( $V_c$ ). The mean values of the above parameters of composites take the following form [10, 11]:

the specific heat:

$$c_c = \frac{V_p c_p \rho_p + (1 - V_p) c_m \rho_m}{\rho_c} \quad (1)$$

the thermal conductivity:

$$\lambda_c = \lambda_m \frac{2\lambda_m + \lambda_p - 2V_p(\lambda_m - \lambda_p)}{2\lambda_m + \lambda_p + V_p(\lambda_m - \lambda_p)} \quad (2)$$

the density:

$$\rho_c = V_p \rho_p + (1 - V_p) \rho_m \quad (3)$$

the heat of solidification:

$$L_c = L(1 - V_{pm}) \quad (4)$$

where: L, solidification heat of the metal matrix;  $V_{pm}$ , mass content of particles.

The data of thermophysical parameters of the components of SiC/359 composites are listed in Table II. The data for 20% SiC/359, which represents the liquid composite with 20% SiC particles, are calculated with Equations 1 to 3. From Table II it is seen that the specific heat of SiC particles is higher than that of 359 alloy melt. Therefore, because of the addition of SiC

TABLE II Data of thermophysical properties

Property	359 (solid)	359 (liquid)	20%SiC/359	SiC
$c(\text{J}/(\text{kg} \cdot \text{K}))$	1084	963	1047	1300
$\lambda(\text{W}/(\text{m} \cdot \text{K}))$	138	121	117	100
$\rho(\text{kg}/\text{m}^3)$	2700	2400	2560	3200
$L(\text{kJ}/\text{kg})$		389		

TABLE III Cooling rate of the materials

Rate	359		10%SiC/359		20%SiC/359	
	No Sr	Sr added	No Sr	Sr added	No Sr	Sr added
$dT/dt$	0.34	0.55	0.78	0.60	1.1	0.81

particles to the base alloy, on one hand the released latent heat by solidification decreases given the reduction of liquid amount in unit volume, on the other hand its effect on temperature decreases given the increase of specific heat. From Equation 4, when  $V_{\text{pm}} = 20\%$ , the latent heat amount of the composite will be decreased to 80% of that of the base alloy. With Equation 2, the calculation result shows that the heat diffusivity  $\lambda_{\text{C}}$  of 20% SiC composite is only slightly lower than that of the 359 (Table II).

Therefore the total amount of heat of the composites is reduced because the latent heat is decreased due to introduction of SiC particles. This explains the reduction of eutectic solidification time ( $\Delta t_{\text{E}}$ ) of SiC/359 composites compared with 359 alloys.

The decrease of undercoolings of metal-matrix composites was also confirmed by Sundarrajan *et al.* [3] through dendrite tip temperature measurements with unidirectional solidification method. It is expected to be caused by the geometrical constraint imposed on primary or eutectic growth by the ceramic fibers or particles. In the presence of fibers or particles, the undercooling at the tip of the freezing phases is primarily due to solute build-up and diffusion in front of the growing tips [3, 12].

The cooling rates of the materials obtained from the cooling curves are shown in Table III. The cooling rates of the composites are slightly higher than those of 359 base alloy. This result supports the observations by other researchers [13, 14].

#### 4.2. Effects of Sr modification on solidification behavior

The process of Sr modification is reported to depress the eutectic temperature by 7 to 9 K in alloy 359. This is also confirmed by this study, as shown in Figs 2 and 5. The mechanism of Sr modification is proposed to be that eutectic Si facets are adsorbed by Sr, which prevents Si from growing on the fast-growing facets [15].

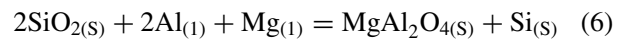
For the SiC particulate reinforced composites, Sr modification can also depress the eutectic temperature, and extend the eutectic solidification time (Figs 5 and 6). However, the eutectic temperature is only depressed by 3 to 5 K, and the eutectic Si is coarser than that in modified 359 (Fig. 7). There may be two reasons: one

is that some strontium may be adsorbed on surfaces of SiC particles, which leads to consumption of strontium in the melt [16]; the other is that SiC particles have the effect of promoting nucleation and growth of Si phases [1, 17, 18]. Because SiC particles are rejected into the liquid by the growing primary  $\alpha$  phases, the remaining eutectic melt is rich in SiC particles. Some SiC particles are indeed connected by silicon phases (Fig. 7).

Wang *et al.* [17], Rohatgi *et al.* [19] and Suery *et al.* [20] have reported the primary Si phase nucleation on SiC particles based on the examination of solidified structure of SiC particulate reinforced hypereutectic Al-Si alloys. It is found in this research that the eutectic Si also could nucleate on SiC particles in hypoeutectic Al-Si alloys. The heterogeneous nucleation mechanism of eutectic Si on SiC particles should be the same to primary Si. It is expected that a semi-coherent relationship exists between the Si and SiC crystals, an orientation relationship described by

$$\begin{aligned} (1\ 1\ 1)_{\text{Si}} // (0\ 0\ 0\ 1)_{\alpha\text{-SiC}} \\ [0\ 1\ 1]_{\text{Si}} // (1\ 1\ \bar{2}\ 0)_{\alpha\text{-SiC}} \end{aligned} \quad (5)$$

will exhibit a relatively small mismatch of  $-6.9\%$  when a match of three Si atoms in Si and every four Si atoms in  $\alpha\text{-SiC}$  [17]. For the fabrication process of SiC<sub>p</sub>/Al-Si composites with pre-oxidized SiC particles, a few nanometers thick of SiO<sub>2</sub> layer will be formed on the surface, and it will react with Al and Mg in the melt to form spinel compound (MgAl<sub>2</sub>O<sub>4</sub>) on the surface.



An orientation relationship, which preserves the hexagonal symmetry across the interface of Si and spinel, is described by

$$\begin{aligned} (1\ 1\ 1)_{\text{Si}} // (1\ 1\ 1)_{\text{MgAl}_2\text{O}_4} \\ [0\ 1\ 1]_{\text{Si}} // [0\ 1\ 1]_{\text{MgAl}_2\text{O}_4} \end{aligned} \quad (7)$$

In this arrangement, every three Si atoms match up with every four Al atoms, with a mismatch of 1% along the three  $\langle 0\ 1\ 1 \rangle_{\text{Si}}$  type directions [17]. Therefore SiC particles can be the substrates of heterogeneous nucleation of eutectic Si in hypoeutectic Al-Si alloys. However, further experimental investigation is necessary to reveal the exact orientation relationships at the interface.

Although strontium can modify eutectic silicon in Al-Si alloy matrix composites, it could not promote an uniform distribution of SiC particles. The particles are still pushed by the  $\alpha$  phase, and distributed between dendrites (Fig. 7). If particles are not rejected by growing solid, particles will be uniformly distributed in the solid phase. Although the solidification rate has some effect on particle distribution, the behavior of ceramic particles in front of the solid  $\alpha$ /liquid interface is mainly determined by the relationship of interfacial energies between the particle/solid/liquid phases [18, 21]. There have been many efforts to date aiming to produce an uniform distribution of SiC particles in SiC/Al-Si composites.

## 5. Conclusions

(1) The eutectic growth temperature of the 10vol% or 20vol% SiC<sub>p</sub>/359 composites modified with Sr lies in the range of 840 to 843 K, which is about 5 to 7 K higher than that of the base alloy with strontium modification. The process of modification depresses the eutectic temperature by 7 to 9 K in the unreinforced 359 alloy, but it has a relatively small effect in depressing the eutectic temperature of the composites.

(2) The eutectic undercooling of the composites is lower than that in 359 alloys. For the same SiC<sub>p</sub>/Al-Si composites, the eutectic undercooling is higher with strontium modification than without. The higher the particle content, the shorter the eutectic solidification time  $\Delta t_E$ .

(3) The solidification time of primary  $\alpha$  dendrites is also shortened because of the presence of the ceramic particles. Measurement of the cooling rate in a given sample reveals that the composites' cooling rate is about 1 K/s, which is higher than that of the base alloy (0.5 K/s) for the same pouring temperature.

(4) The primary dendrites of the composites are finer than those in the base alloy. Moreover, strontium modification has a refining effect on eutectic silicon for the SiC<sub>p</sub>/Al-Si composites, and eutectic Si phase can nucleate on SiC particles.

## References

1. A. MORTENSEN and I. JIN, *Inter. Mat. Rev.* **37** (1992) 101.
2. S. WU, N. HUANG and P. AN, *Trans. Nonferrous Met. Soc. China* **9** (1999) 524.

3. A. SUNDARRAJAN, A. MORTENSEN, T. Z. KATTAMIS and M. C. FLEMINGS, *Acta. Mater.* **46** (1998) 91.
4. A. MORTENSEN, *Mater. Sci. Eng. A* **173** (1993) 205.
5. B. R. KROHN, *Modern Casting* **75** (1985) 21.
6. G. K. SIGWORTH, *Am. Foundrymen's Soc. Trans.* **91** (1983) 7.
7. N. TENEKJEV and J. E. GRUZLESKI, *Am. Foundrymen's Soc. Trans.* **98** (1991) 1.
8. S. GOWRI and F. H. SAMUEL, *Metall. Trans. A* **23A** (1992) 3369.
9. H. NAKAE and S. WU, *Key Eng. Mater.* **127-131** (1997) 503.
10. J. BRASZCZYNSKI, *Mat. Sci. & Eng. A* **135** (1991) 105.
11. J. BRASZCZYNSKI and A. ZYSKA, *ibid.* **278** (2000) 195.
12. D. LIANG, Y. BAYRAKTAR and H. JONES, *Acta Metall. Mater.* **43** (1995) 579.
13. G. S. HANUMANTH and G. A. IRONS, Proc. 1st Inter. Conf. on Process. Mat. For Properties, edited by H. Henein and T. Oki (TMS, 1993) p. 29.
14. W. R. HOOVER, "Fabrication of Particulates Reinforced Met. Comp.," edited by J. Masounave and F. G. Hamel (ASM Inter., Metals Park, OH, 1990) p. 115.
15. K. SONG and H. NAKAE, *J. Japan Light Met. Soc.* **43** (1993) 484.
16. S. WU and H. NAKAE, *J. Mater. Sci. Lett.* **18** (1999) 321.
17. W. WANG, F. AJERSCH and J. P. A. LÖFANDER, *Mat. Sci. & Eng. A* **187** (1994) 65.
18. H. NAKAE and S. WU, *ibid.* **252** (1998) 232.
19. P. K. ROHATGI, F. M. YARANDI and Y. LIU, Metal Comp. Proc. Int. Symp. Advanced in Cast Reinforced Metal Composites (1988) p. 249.
20. M. SUERY and L. LAJOYE, "Solidification of Metal Matrix Composites" (TMS-ASM Committee, TMS Publication, 1989) p. 171.
21. S. WU, H. NAKAE, T. KANNO and Y. YOU, *J. Mater. Sci.* **36** (2001) 225.

*Received 8 March*

*and accepted 13 November 2001*